CHEMISTRY
A EUROPEAN JOURNAL

Water Cluster Growth in Hydrophobic Solid Nanospaces

Tomonori Ohba, Hirofumi Kanoh, and Katsumi Kaneko*[a]

Abstract: The growth mechanism of water clusters in carbon nanopores is clearly elucidated by in situ small-angle X-ray scattering (SAXS) studies and grand canonical Monte Carlo (GCMC) simulations at 293–313 K. Water molecules are isolated from each other in hydrophobic nanopores below relative pressures (P/P_0) of 0.5. Water molecules associate with each other to form clusters of about 0.6 nm in size at $P/P_0 = 0.6$, accompanied by a remarkable aggregation of these clusters. The complete filling of carbon nanopores finishes at about $P/P_0 = 0.8$. The correlation length analysis of SAXS profiles leads to the proposal of a growth mechanism for these water clusters and the presence of the critical cluster size of 0.6 nm leads to extremely stable clusters of water molecules in hydrophobic nanopores. Once a cluster of the critical size is formed in hydrophobic nanopores, the predominant water adsorption begins to fill carbon nanopores.

Keywords: cluster compounds · hydrophobicity · nanostructures · water chemistry

Introduction

Water is indispensable to living cells.[1–3] Although lipid membrane bilayers exhibit highly limited water permeability, water can penetrate the cells.[4–9] The presence of water channels in membranes was already predicted in the 1950s. The narrowest water-channel pore size is presumed to be 0.3 nm, which is only slightly larger than the diameter of a water molecule (0.28 nm).[10–12] The membrane with a water channel has hydrophobic properties and the presence of active sites in the narrowest pores is assumed. Water molecules are supposed to be stable in such hydrophobic nanoscale spaces. Hence, the hydrophobicity-gain mechanism of water molecules in nanopores needs to be elucidated. Furthermore, the structure of water confined in nanoscale spaces has been presumed to be different from that of the bulk. For instance, water molecules in nanopores cannot form large clusters that are larger than the nanopore width due to the size restriction, while in the bulk vapor clusters are not formed as evidenced by IR spectroscopy.[13,14] Instead they associate to form larger clusters on condensation. Thus, the properties and structures of water in hydrophobic nanopores have been actively studied.[15–24]

[a] Dr. T. Ohba, Dr. H. Kanoh, Prof. K. Kaneko
Department of Chemistry, Faculty of Science
Chiba University, 1–33 Yayoi, Inage, Chiba 263–8522 (Japan)
Fax: (+81) 43-290-2788
E-mail: kaneko@pchem2.s.chiba-u.ac.jp

Graphite carbon materials are typically hydrophobic. The simplest evidence for the hydrophobicity of graphite carbon materials is given by the fact that the contact angle of water on a graphite basal plane is in the range of 50–90°, though the contact angle value is sensitive to surface contamination.[25,26] Thus, study of water adsorption in carbon nanopores can be associated with the fundamental subject of water in hydrophobic nanoenvironments. Many studies on water adsorption in carbon nanopores have given the current mechanism that oxygen-containing groups at the surface of the grpahite induce water adsorption.[27–39] However, it is also known that some nanoporous carbon materials that have been heat-treated in an inert atmosphere or treated in hydrogen provide a characteristic adsorption isotherm;[40] the water adsorption below $P/P_0 = 0.4$ is zero, but a marked increase occurs just above $P/P_0 = 0.5$. Consequently, we need a new mechanism for water adsorption in carbon nanopores that are free of surface functional groups; this should be helpful in understanding the stability of water in the channels of membranes. Recent molecular simulation studies pointed out that graphite slit nanopores which are free of surface functional groups give a predominant adsorption uptake near $P/P_0 = 0.5$.[41–43] In particular Ohba et al. showed the reason why water molecules are stabilized in graphite nanopores.[45] With in situ X-ray diffraction and in situ small-angle X-ray scattering (SAXS), Iiyama et al. showed clear evidences that water molecules confined in carbon nanopores have an solid-like structure.[17,46,47] Accordingly, a combined study on water adsorption in carbon nanopores

DOI: 10.1002/chem.200400918

with grand canonical Monte Carlo (GCMC) simulation and in situ SAXS can elucidate the cluster structure of water molecules and the growth mechanism of water nanoclusters in hydrophobic nanopores. This paper describes the critical water cluster size for cluster growth and the molecular mechanism of the cluster growth in the nanopores.

Results and Discussion

The experimental adsorption isotherms of water at 293, 303, and 313 K together with a simulated isotherm at 303 K are shown in Figure 1. These experimental isotherms almost perfectly coincide with each other, showing an adsorption hysteresis loop. On the other hand, the simulated isotherm has no adsorption hysteresis, agreeing with the desorption branch of the experimental isotherm. The simulated isotherm is obtained under complete equilibrium conditions and, thus, the desorption branch of the experimental isotherm should reflect the equilibrium process. Therefore, we cannot describe the experimental adsorption branch over the whole P/P_0 range by GCMC simulation. As experimental adsorption and desorption branches overlap each other up to a 0.08 fractional filling (ϕ), the GCMC simulation data below $\phi=0.08$ must be referable. Consequently, we will discuss the GCMC simulation data at $\phi=0.06$. However, we need information on the abrupt adsorption jump in the adsorption branch. The in situ SAXS profiles at 303 K on adsorption and desorption branches coincided with each other until $\phi=0.24$, although those data are not shown here. Accordingly, we can use the GCMC simulation data at $\phi=0.24$ for determining molecular states on the adsorption branch. Snapshots of the GCMC simulated isotherm at $\phi=0.06$, 0.24, and 0.60 are shown in Figure 2. The experimental adsorption amount of the desorption branch near $P/P_0=0.5$ is in the range of $\phi=0.06$–0.24, while $\phi=0.60$ corresponds to that at $P/P_0=0.6$. That is, snapshots at $\phi=0.06$ and 0.24 express adsorption states before and just after the adsorption jump of the isotherm. Figure 3 shows the cluster distribution determined from the snapshots in Figure 2. The peak positions at $\phi=0.06$, 0.24 and 0.60 are 7, 8, and 13, respectively, indicating the increase of the cluster size with the filling. Some clusters consisting of less than ten water molecules are observed at $\phi=0.06$; water molecules already form clusters of considerable size even at $\phi=0.06$. They rarely form clusters below $\phi=0.02$ and in such cases they are mostly isolated from each other, although the snapshot is not shown. Accordingly, water clusters grow gradually with the increase in P/P_0 before the adsorption jump of the isotherm. The snapshot at $\phi=0.24$ expresses a different feature from that of $\phi=0.06$; clusters merge with each other to form a partially continuous adsorbed layer. Thus, the greater the filling, the broader the cluster-size distribution. The peak of the

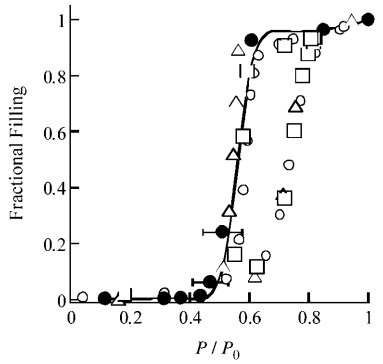

Figure 1. Adsorption isotherms of water at 293 K (○), 303 K (△), and 313 K (□) together with the simulated isotherm at 303 K (●).

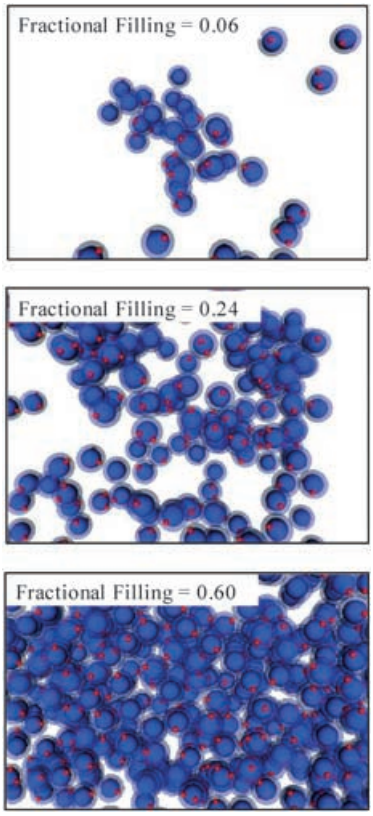

Figure 2. Snapshots at $\phi=0.06$, 0.24, and 0.60. Blue circle: oxygen, red circle: hydrogen.

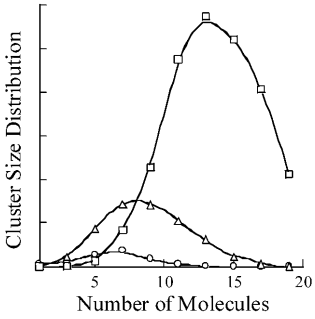

Figure 3. Cluster size distributions of water at $\phi=0.06$ (○), 0.24 (△), and 0.60 (□).

cluster size distribution at $\phi=0.60$ evidently shift to the right side, as mentioned above, which shows the growth of clusters.

The growth of water clusters shown by GCMC simulation can be experimentally verified by in situ SAXS. The SAXS profiles at $\phi=0.4$ are shown in Figure 4a. Then we applied

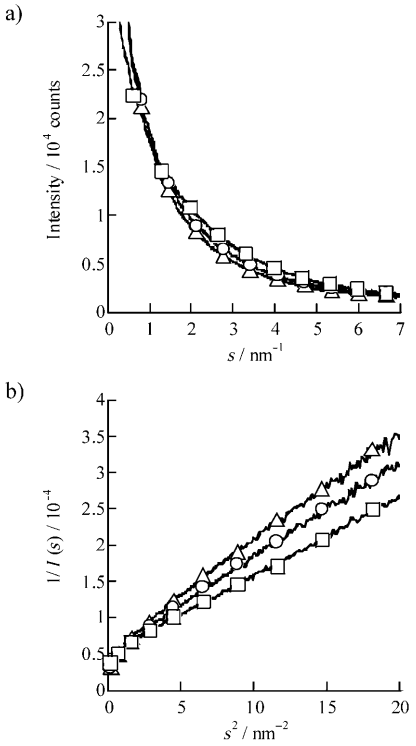

Figure 4. SAXS profiles at $\phi=0.4$ (a) and the OZ plots (b). ○: 293 K, △: 303 K, and □: 313 K.

an Ornstein–Zernike (OZ) analysis to these SAXS profiles. Figure 4b shows linear OZ plots for the SAXS profiles. Consequently, the correlation length can be determined. The correlation lengths versus the fractional filling at different temperatures are shown in Figure 5. The correlation length

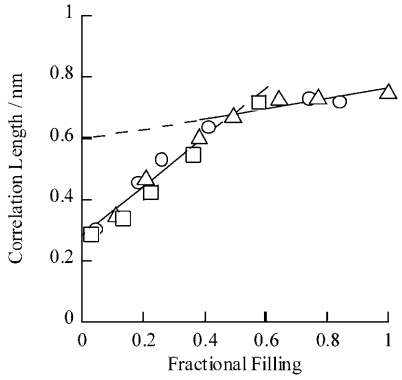

Figure 5. Correlation lengths of adsorbed water at 293 K (○), 303 K (△), and 313 K (□).

gives the direct information of average cluster size. Thus, the water cluster growth mechanism in hydrophobic nanopores can be shown experimentally by using the variation of the correlation length with the fractional filling. The correlation length versus ϕ relationship is independent of the temperature, because the data at different temperatures form a common linear relation. This linear relationship bends downward at $\phi=0.5$, and in the small ϕ region is has been extrapolated to $\phi=0$. The intercept of the steep linear relation corresponds to the correlation length of 0.3 nm, which originates from the water–carbon distance ($\sigma_{sf}=0.33$ nm). Therefore, water molecules are initially adsorbed on the nanopore wall, and then they associate with each other to form the clusters. The linear increase of the correlation length with ϕ stems from the growth of unit clusters below $\phi=0.5$. On the other hand, the linear relationship above $\phi=0.5$ comes from the merging of unit clusters, because the merging can be regarded as the filling of intercluster voids with water molecules and thereby the correlation length does not increase so much. Consequently, the extrapolation of the linear relationship in the higher fractional filling range to $\phi=0$ provides the average size of the unit cluster, which should be essential for the induction of the predominant water adsorption. Hence, this unit cluster size is named the critical cluster size in this article. The correlation length at the intercept is 0.6 nm, which corresponds to 8–10 associated water molecules under the assumption of the spherical cluster shape.[48–51] That is, clusters such as octamers to decamers of water molecules have enough hydrophobicity to be stably adsorbed in carbon nanopores, agreeing with the prediction by the preceding interaction potential calculation. Furthermore, the correlation length corresponding to the bending point of the linear relationship indicates the cluster size (~0.7 nm) of which clusters initiate bridging to form uniform adsorbed layers in the nanopores.

The schematic model of the water cluster growth is shown in Figure 6. Isolated molecules associate with each other to form unit clusters of the critical size of 0.7 nm, as shown in Figure 6a,b. Then, unit clusters bridge each other to form an adsorbed layer with interstices, as shown by Figure 6c. Finally water molecules are adsorbed in the interstices.

Thus, snapshot analysis of GCMC simulation and in situ SAXS can determine the critical unit size of the water clusters that gain a sufficient hydrophobicity and give the molecular basis for the adsorption jump in the water adsorption isotherm on nanoporous carbon near $P/P_0=0.5$. At the same time, the growth process of the clusters can be shown. The hydrophobicity gain by the water cluster formation should be studied with the relevance to water channels in the cell membrane in future.

Experimental and Simulated Section

Pitch-based activated carbon fiber (ACF P20) was used as the model graphitic nanoporous system, because previous studies with X-ray photoelectron spectroscopy, magnetic susceptibility, X-ray diffraction, and en-

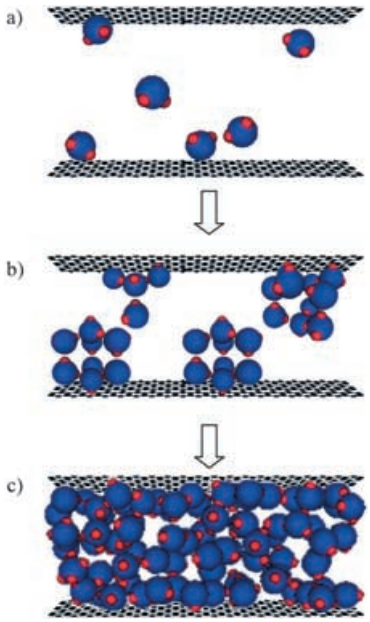

Figure 6. Adsorbed water models. a) isolated molecules, b) unit cluster formation, and c) filling of interstices among clusters. Blue circle: oxygen, red circle: hydrogen.

thalpy of immersion confirm that ACF P20 has a good nanographitic structure.[52–54] Water adsorption isotherms were measured volumetrically every 10 K in the temperature range 293–303 K. The SAXS of water-adsorbed ACF P20 was measured by using $Cu_{K\alpha}$ radiation. The SAXS profiles were measured for the angle range 0.2–7.0°. The SAXS experiments were performed on apparatus that had a two-axial and three-slit system. ACF P20 was heat-treated at 383 K below 1 mPa for 2 h prior to the adsorption and in situ SAXS measurements. The correlation length was obtained from the Ornstein–Zernike (OZ) analysis of SAXS profile near-scattering factor $s=0$ using Equation (1).[55]

$$I(s) = \frac{I(0)}{1+\xi^2 s^2} \tag{1}$$

Here, $I(s)$, $I(0)$, and ξ are the scattering intensity at s, the scattering intensity at $s=0$, and the OZ correlation length, respectively. The goodness of the OZ relationship can be examined by the following OZ plot [Eq. (2)]:

$$\frac{1}{I(s)} = \frac{1}{I(0)} + \frac{\xi^2}{I(0)} s^2 \tag{2}$$

The linear plot of $I(s)^{-1}$ versus s^2 provides both $I(0)$ and ξ. Here ξ can be a scale of the size of water clusters in the carbon nanopores in the initial stage of adsorption. Although $I(0)$ can give information on the cluster–cluster structure, we will focus on the change of ξ with water adsorption in this article.

As water molecules form hydrogen bonds, the intermolecular interaction of water molecules should be approximated by the sum of the dispersion interaction and the electrostatic interaction between partial charges on the atomic sites of a water molecule, as given by the TIP-5P model [Eq. (3)].[56]

$$\phi_{ff}(r) = 4\varepsilon_{ff}\left[\left(\frac{\sigma_{ff}}{r}\right)^{12} - \left(\frac{\sigma_{ff}}{r}\right)^{6}\right] + \sum_{i}^{4}\sum_{j(\neq i)}^{4} \frac{1}{4\pi\varepsilon_0}\frac{q_i q_j}{r_{ij}} \tag{3}$$

Here ε_{ff} and σ_{ff} are the intermolecular potential-well depth ($\varepsilon_{ff}/k_B = 80.5$ K) and the effective diameter ($\sigma_{ff}=0.312$ nm), respectively. The absolute value of the effective electric charges of the hydrogen atom and the oxygen lone pair ($|q_i|$) are 3.86×10^{-20} C. The distances between the H–O and O-lone pair are 0.0957 and 0.0700 nm, respectively.

On the other hand, the interaction of a water molecule with the graphite surface can be described by Steele's 10-4-3 potential function,[57] Equation (4) in which A is $2\pi\sigma_{sf}^2\varepsilon_{sf}\rho\Delta_C$, z is the distance of a molecule from the graphite surface, ρ is the carbon atomic number density, Δ_C is the interlayer distance of the graphite, and ε_{sf} and σ_{sf} are fitted parameters of the water-carbon potential depth and effective diameter, respectively, which were obtained using the Lorentz–Berthelot rules ($\varepsilon_{sf}/k_B = 49.3$ K, $\sigma_{sf}=0.327$ nm).

$$\phi_{sf}(z) = A\left[\frac{2}{5}\left(\frac{\sigma_{sf}}{z}\right)^{10} - \left(\frac{\sigma_{sf}}{z}\right)^{4} - \frac{{\sigma_{sf}}^4}{3\Delta_C(z+0.61\Delta_C)^3}\right] \tag{4}$$

In the case of the graphite slit pore, the interaction of the water molecule with the pore is expressed by the sum of the interaction potentials of the water molecule with both graphite walls, as given by Equation (5).

$$\phi_p = \phi_{sf}(z) + \phi_{sf}(H-z) \tag{5}$$

Here H is the physical slit pore width, which is the internuclear distance between opposite graphite walls. The physical slit pore width is associated with the effective pore width w, which is approximated by the experimentally determined pore width [Eq. (6)].[58]

$$w = H-(2z_0-\sigma_{ff}) \qquad z_0 = 0.856\sigma_{sf} \tag{6}$$

Here, z_0 is the closest contact distance between the water molecule and the graphite pore wall.

The water adsorption isotherm of the graphite slit pore at 303 K was simulated with the established grand canonical Monte Carlo (GCMC) procedure.[59,60] We used a rectangular cell $l\times l\times w$ for the calculation to determine which size is replicated two-dimensionally to form an infinite slit-shaped pore. Here, the values of l and w are 10 and 1.1 nm, respectively.

Acknowledgements

This work was funded by Research Fellowships of the Japan Society for the Promotion of Science (JSPS) for Young Scientists and a Grant-in-Aid for Scientific Research (S) (No. 15101003) by JSPS.

[1] P. Agre, D. Brown, S. Nielsen, *Curr. Opin. Cell Biol.* **1995**, *7*, 472.
[2] L. S. King, S. Nielsen, P. Agre, *J. Clin. Invest.* **1996**, *97*, 2183.
[3] P. Agre, D. Kozono, *FEBS Lett.* **2003**, *555*, 72.
[4] K. Murata, K. Mitsuoka, T. Hirai, T. Walz, P. Agre, J. B. Heymann, A. Engel, Y. Fujiyoshi, *Nature* **2000**, *407*, 599.
[5] Y. Fujiyoshi, K. Mitsuoka, B. L. Groot, A. Philippsen, H. Grubmüller, P. Agre, A. Engel, *Curr. Opin. Struct. Biol.* **2002**, *12*, 509.
[6] M. R. Cho, D. W. Knowles, B. L. Smith, J. J. Moulds, P. Agre, N. Mohandas, D. E. Golan, *Biophys. J.* **1999**, *76*, 1136.
[7] G. P. Nicchia, A. Frigeri, B. Nico, D. Ribatti, M. Svelto, *J. Histochem. Cytochem.* **2001**, *49*, 1547.
[8] P. Jedlovszky, M. Mzei, *J. Chem. Phys.* **1999**, *111*, 10770.
[9] R. J. Law, M. S. P. Sansom, *Curr. Biol.* **2002**, *12*, R250.
[10] A. C. Belch, M. Berkowitz, *Chem. Phys. Lett.* **1984**, *113*, 278.
[11] W. L. Jorgensen, *J. Am. Chem. Soc.* **1981**, *103*, 335.
[12] Y. Guissani, B. Guillot, *J. Chem. Phys.* **1993**, *98*, 8221.
[13] D. Eisenberg and W. Kauzmann, *The Structure and Properties of Water*, Clarendon Press, Oxford, UK, **1969**.
[14] W. S. Benedict, H. H. Claassen, J. H. Shaw, *J. Res. Natl. Bur. Stand.* **1952**, *49*, 91.

[15] J. Alcaniz-Monge, A. Linares-Solano, B. Rand, *J. Phys. Chem. B* **2001**, *105*, 7998.
[16] J. K. Brennan, K. T. Thomson, K. E. Gubbins, *Langmuir* **2002**, *18*, 5438.
[17] T. Iiyama, M. Ruike, K. Kaneko, *Chem. Phys. Lett.* **2000**, *331*, 359.
[18] K. Kaneko, Y. Hanzawa, T. Iiyama, T. Kanda, T. Suzuki, *Adsorption* **1999**, *5*, 7.
[19] K. A. Sharp, B. Madan, *J. Phys. Chem. B* **1997**, *101*, 4343.
[20] T. Werder, J. H. Walther, R. L. Jaffe, T. Halicioglu, P. Koumoutsakos, *J. Phys. Chem. B* **2003**, *107*, 1345.
[21] M. Ehrl, H. W. Augustin, F. W. Deeg, C. Brauchle, *Chem. Phys. Lett.* **2002**, *355*, 19.
[22] J. Alcaniz-Monge, A. Linares-Solano, B. Rand, *J. Phys. Chem. B* **2002**, *106*, 3209.
[23] T. Köddermann, F. Schlte, M. Huelsekoph, R. Ludwig, *Angew. Chem.* **2003**, *115*, 5052; *Angew. Chem. Int. Ed.* **2003**, *42*, 4904.
[24] K. Koga, G. T. Gao, H. Tanaka, X. C. Zeng, *Nature* **2001**, *412*, 802.
[25] M. E. Shrader, *J. Phys. Chem.* **1975**, *79*, 2508.
[26] M. Lundgren, N. L. Allan, T. Cosgrove, and N. George, *Langmuir* **2002**, *18*, 10462.
[27] W. H. Lee, P. J. Reucroft, *Carbon* **1999**, *37*, 7.
[28] Y. Kaneko, M. Abe, K. Ogino, *Colloids Surf.* **1989**, *37*, 211.
[29] M. Jorge, C. Schumacher, N. A. Seaton, *Langmuir* **2002**, *18*, 9296.
[30] A. Striolo, K. E. Gubbins, A. A. Chialvo, P. T. Cummings, *Mol. Phys.* **2004**, *102*, 243.
[31] I. I. Salame, T. J. Bandosz, *Langmuir* **1999**, *15*, 587.
[32] A. Lopez, T. Bitzer, T. Heller, N. V. Richardson, *Surf. Sci.* **2001**, *473*, 108.
[33] F. Julien, M. Baudu, M. Mazet, *Water Res.* **1998**, *32*, 3414.
[34] D. Mowla, D. D. Do, K. Kaneko, *Chem. Phys. Carbon* **2003**, 28, 229.
[35] J. Phillips, D. Kelly, L. Radovic, F. Xie, *J. Phys. Chem. B* **2000**, *104*, 8170.
[36] I. I. Salame, A. Bagreev, and T. J. Bandosz, *J. Phys. Chem. B* **1999**, *103*, 3877.
[37] R. S. Vartapentyan, A. M. Voloshchuk, A. A. Isirikyan, N. S. Polyakov, Y. I. Tarasevich, *Colloids Surf. A* **1995**, *101*, 227.
[38] J. Choma, W. Burakiewicz-Mortka, M. Jaroniec, Z. Li, J. Klinik, *J. Colloid Interface Sci.* **1999**, *214*, 438.
[39] F. Rodoriguez-Reinoso, M. Molina-Sabio, M. T. González, *Langmuir* **1997**, *13*, 2354.
[40] T. Ohkubo, C. -M. Yang, E. Raymundo-Pinero, Linares-Solano, K. Kaneko, *Chem. Phys. Lett.* **2000**, *329*, 71.
[41] E. A. Müller, F. R. Hung, K. E. Gubbins, *Langmuir* **2000**, *16*, 5418.
[42] A. Striolo, K. E. Gubbins, A. A. Chialvo, P. T. Cummings, *Mol. Phys.* **2004**, *102*, 243.
[43] A. M. Slasli, M. Jorge, F. Stoeckli, N. A. Seaton, *Carbon* **2003**, *41*, 479.
[44] M. Jorge, C. Schmucher, N. A. Seaton, *Langmuir* **2002**, *18*, 9296.
[45] T. Ohba, H. Kanoh, K. Kaneko, *J. Am. Chem. Soc.* **2004**, *126*, 1560.
[46] T. Iiyama, K. Nishikawa, T. Otowa, K. Kaneko, *J. Phys. Chem.* **1995**, *99*, 10075.
[47] T. Iiyama, K. Nishikawa, T. Suzuki, K. Kaneko, *Chem. Phys. Lett.* **1997**, *274*, 152.
[48] K. Liu, M. G. Brown, C. Carter, R. J. Saykally, J. K. Gregory, D. C. Clary, *Nature* **1996**, *381*, 501.
[49] S. Maheshwary, N. Patel, N. Sathyamurthy, A. D. Kulkarni, S. R. Gadre, *J. Phys. Chem. A* **2001**, *105*, 10525.
[50] F. N. Keutsh, R. J. Saykally, *Proc. Natl. Acad. Sci. USA* **2001**, *98*, 10533.
[51] M. G. Brown, F. N. Keutsch, R. J. Saykally, *J. Chem. Phys.* **1998**, *109*, 9645.
[52] M. El-Merraoui, H. Tamai, H. Yasuda, T. Kanata, J. Mondori, K. Nadai, K. Kaneko, *Carbon* **1998**, *36*, 1769.
[53] T. Enoki, N. Kawatsu, Y. Shibayama, H. Sato, R. Kobori, S. Maruyama, K. Kaneko, *Polyhedron* **2001**, *20*, 1311.
[54] S. Shin, J. Jang, S.-H. Yoon, I. Mochida, *Carbon* **1997**, *35*, 1739.
[55] L. S. Ornstein, F. Zernike, *Proc. K. Ned. Acad. Wet.* **1914**, *17*, 793.
[56] M. W. Mahoney, W. L. Jorgensen, *J. Chem. Phys.* **2000**, *112*, 8910.
[57] W. A. Steele, *Surf. Sci.* **1973**, *36*, 317.
[58] K. Kaneko, R. F. Cracknell, D. Nicholson, *Langmuir* **1994**, *10*, 4606.
[59] T. Ohba, H. Kanoh, K. Kaneko, *J. Phys. Chem. B* **2004**, *108*, 14964.
[60] T. Ohba, K. Kaneko, *Langmuir* **2001**, *17*, 3666.

Received: September 7, 2004
Revised: March 23, 2005
Published online: June 1, 2005